Abstract

The variability of the atmospheric concentration of the ^{7}Be and ^{210}Pb radionuclides is strongly linked to the origin of air masses, the strength of their sources and the processes of wet and dry deposition. It has been shown how these processes and their variability are strongly affected by climate change. Thus, a deeper knowledge of the relationship between the atmospheric radionuclides variability measured close to the ground and these atmospheric processes could help in the analysis of climate scenarios. In the present study, we analyse the atmospheric variability of a 14-year time series of ^{7}Be and ^{210}Pb in a Mediterranean coastal city using a synergy of different indicators and tools such as: the local meteorological conditions, global and regional climate indexes and a lagrangian atmospheric transport model. We particularly focus on the relationships between the main pathways of air masses and sun spots occurrence, the variability of the local relative humidity and temperature conditions, and the main modes of regional climate variability, such as the North Atlantic Oscillation (NAO) and the Western Mediterranean Oscillation (WeMO).

The variability of the observed atmospheric concentrations of both ^{7}Be and ^{210}Pb radionuclides was found to be mainly positively associated to the local climate conditions of temperature and to the pathways of air masses arriving at the station. Measured radionuclide concentrations significantly increase when air masses travel at low tropospheric levels from central Europe and the western part of the Iberian Peninsula, while low concentrations are associated with westerly air masses. We found a significant negative correlation between the WeMO index and the atmospheric variability of both radionuclides and no significant association was observed for the NAO index.

1. Introduction

The air concentrations of radioisotopes with a relatively short lifetime, such as ^{210}Pb and ^{7}Be, have long been recognized as useful proxies to study atmospheric transport and the origin of air masses (e.g. Vecchi and Valli, 1997; Leppanen et al., 2010; Baskaran et al., 2011; Piñero-García et al., 2015). ^{7}Be is a cosmogenic isotope with a half-life time ($T_{1/2}$) of 53.6 days (e.g. Papastefanou and Ioannidou, 1995). It is produced in the atmosphere as a result of the spallation of nitrogen and oxygen nuclei by components of an atmospheric cascade induced by the Galactic Cosmic Rays (GCR; e.g. Dorman, 2004; Leppanen et al., 2010). ^{7}Be is mainly produced in the stratosphere, but also in the highest levels of the troposphere (e.g. Johnson and Viezee, 1981; Usoskin and Kovaltsov, 2008; Leppanen et al., 2010). GCR are modulated by the solar magnetic activity, so that they typically increase the concentration of ^{7}Be when the solar activity is minimal, and vice versa (Forbush, 1954). ^{7}Be is then adsorbed by atmospheric aerosols and it can be transported within different atmospheric layers and to the ground level as a result of vertical down mixing (e.g. Papastefanou and Ioannidou, 1995; Winkler et al., 1998). Previous studies have already described the connection between solar activity and the concentration of ^{7}Be in the lower troposphere (Azahra et al., 2003; Aldahan et al., 2001; Kikuchi et al., 2009). In addition to its production, the presence of this cosmogenic nuclide near the surface can be mainly modulated on daily time scale by (i) the wet scavenging, (ii) the exchange between the stratosphere and the troposphere (STE), (iii) the tropospheric vertical mixing and (iv) the horizontal transport across different latitudes (Feely et al., 1989). The complexity of the interactions of all these mechanisms makes difficult to completely understand the atmospheric variability of ^{7}Be concentrations measured at the surface layer in ground-based stations.

^{210}Pb ($T_{1/2}$ = 22.3 years) is a terrestrial radionuclide whose concentration derives from the natural decay of ^{222}Rn ($T_{1/2}$ = 3.8 days), which in turn emanates from the Earth's surface (Porstendorfer, 1994). Due to its long-lasting activity, atmospheric ^{210}Pb concentration can increase with height and can reach high values in the stratosphere (Jacobi, 1963). Piliposian and Appleby (2003) showed that over large continental land masses the ^{210}Pb inventory is predominantly located in the troposphere, but that as the air column moves out over the sea, the stratospheric inventory continues to increase over large distances and is an important factor controlling long-range transport. Although data of atmospheric ^{210}Pb is rather sparse (Kirpa and Sarin, 2012), it is largely used to calculate the rate of sediment accumulation and mixing in lakes, estuaries, marsh, and coastal areas (Bonotto and Vergotti, 2015).

Both radionuclides can get attached to aerosols short after they are produced, being excellent tracers of the atmospheric circulation, including the mixing and transport of air masses and aerosols (e.g. Baskaran et al., 1993; Baskaran, 2011; Tositti et al., 2014; Piñero-García et al., 2015). Recently, the simultaneous measurement of ^{7}Be and ^{210}Pb, together with the calculation of their ratio ^{7}Be/^{210}Pb, has been used for improving the understanding of ozone variability in the high-troposphere and the intrusion of air masses from northern Africa to southern Europe, given that they are diagnostic indicators of horizontal and vertical transport processes (e.g. Gordo et al., 2015; Lee et a., 2015). The atmospheric deposition of ^{7}Be and ^{210}Pb mainly depends on the presence of atmospheric gas and aerosol particles and the occurrence of precipitation (Papastefanou and Ioannidou, 1995). On the other hand, the climate variability has been found to strongly modulate the effect of precipitation on the deposition of atmospheric elements (Izquierdo et al., 2014). This means that the inter-annual characterization of the atmospheric variability of these radionuclides could also be used as a proxy to understand and model the variability of climate itself. The dependence from large circulation patterns implies that the teleconnections could generally lead to air masses transporting atmospheric particles from sources with different emission characteristics (Leppanen et al., 2012; Izquierdo et al., 2014). Particularly, the North Atlantic Oscillation (NAO) mode has been found to be linked to the inter-annual variability of precipitation, dust transport and stratospheric intrusion in the Euro-Mediterranean basin (e.g. Meehl and van Loon, 1979; Rodó et al., 1997; Cristofanelli et al., 2006; Izquierdo et al., 2014). Leppanen et al. (2012) found that the ^{7}Be activities in the North of Europe were mainly modulated by the NAO at inter-annual scales. In addition, the Western Mediterranean Oscillation (WeMO) was recently proposed as an active modulator of precipitation in the Mediterranean basin of the Iberian Peninsula, where the correlation with the NAO is rather weak (Martín-Vide and Lopez-Bustins, 2006; Izquierdo et al., 2014).

The variability of the atmospheric components has been studied with respect to global and regional climate indexes (e.g. Leppanen et al., 2012; Izquierdo et al., 2014; Piñero-Garcia et al., 2015) because changes happening on local scales could be driven by changes occurring on regional/global basis and vice versa (e.g. Galmarini and Thunis, 1999; Galmarini, Michelutti and Thunis, 2000).

In the present study, we analyze two 14-year time series of atmospheric ^{7}Be and ^{210}Pb concentrations measured in the city of Barcelona, in northeastern Spain. The present work aims to understand the variation of the radionuclide concentrations using a multi-scale approach from local to global atmospheric patterns. We use different indicators and tools in order to understand their seasonal and inter-annual atmospheric variability at different spatio-temporal scales. We also describe the relationship between the inter-annual variability of ^{7}Be and the number of sun spots, as well as the influence of the local climate variability on the seasonal ^{7}Be and ^{210}Pb evolution, with particular emphasis on the local temperature (T) and relative humidity (RH) variability. In addition, we analyze the relationship between the monthly values of ^{7}Be and ^{210}Pb and key regional climate indexes such as the WeMO and the NAO.

The methodology used in the present study is described in Section 2 as follows: 2.1) the measurement station, where the atmospheric radionuclides concentrations have been measured; 2.2) the air sampling technique and the γ spectrometry method used for the measurements of the radionuclides concentrations; 2.3) the atmospheric transport model used to calculate the back trajectories of air masses; and 2.4) the astronomical and climate indexes used for the correlation analysis. In Section 3, results describing the seasonal and inter-annual atmospheric variability of ^{7}Be and ^{210}Pb are presented in relation with the climate indexes and the origin of air masses arriving at the sampling station. Results are finally discussed and summarized in sections 4 and 5.

2. Methods

2.1 The sampling site: Barcelona, Spain

Atmospheric levels of ^{7}Be and ^{210}Pb were measured at 65 meters above the mean sea level (m a.s.l.) at the top of a building in Barcelona (BCN; population 1,500,000; latitude 41.38N; longitude 2.12E, 35 m a.s.l.). The city is characterized by a Mediterranean climate (defined as Csa in the Köppen classification, Kottek et al., 2006), between the arid regime of northern Africa and the temperate and rainy climate of central Europe (Dall'osto et al., 2013). Several authors (e.g. Millan et al., 1997; Soriano et al., 2001; Rodriguez et al., 2002; Jorba et al., 2004; Dall'osto et al. 2013) have characterized the main factors modulating the climate in the western Mediterranean. Among them: (i) the influence of the Azores high; ii) the mountain ranges surrounding the Mediterranean coast; iii) the influence of the Iberian and Saharan thermal pressure lows; iv) the intense sea breeze system; v) the scarce summer precipitation; and vi) the large seasonal differences in T, RH and rainfall. Jorba et al. (2004) characterized the main large-scale transport modes to BCN in the low- and mid-troposphere, which can be divided in three distinctive types of westerly wind regimes: fast westerlies, westerlies and slow westerlies. No significant influence of African winds has been reported by Jorba et al. (2004) in BCN at these heights. From a geographical point of view, BCN is 100 km to the south of the Pyrenees, a 500 km wide mountain range with several peaks above 3000 m. In addition, note that several authors (e.g. Reiter, 1991; Stohl et al., 2000; Zanis et al., 2003; Cristofanellli et al., 2006; Lee et al., 2007) have shown the role of the lower stratosphere and the upper troposphere in determining the concentration of radionuclides in high mountain ranges such as the Alps, but this effect have not been described yet for the particular case of the Pyrenees.

2.2 Atmospheric ^{7}Be and ^{210}Pb concentration measurements

Atmospheric ^{7}Be and ^{210}Pb is measured at the Institute of Energy Technologies of the Universitat Politècnica de Catalunya (INTE-UPC) since January 2001 (Valles et al., 2009). A sampler pump (ASS-500 station) is used to make a maximum flow rate of 800 m^3 h^{-1} through G3 polypropylene filters with a size of 44 x 44 cm^2 and 93% collection efficiency, with an average weekly volume ranging between $70 \cdot 10^3$ m^3 and $120 \cdot 10^3$ m^3. Sampled filters, after being folded and pressed to obtain a minimum surface area of about 8 x 8 cm^2, with the active area facing inwards, are analyzed by γ spectrometry with two Canberra Hyperpure Germanium (HPGe) coaxial detectors model GX4020 and GX3020, equipped with a cryostat with Carbon Epoxy window and a cryostat with a Be window, respectively. Detectors present nominal relative efficiencies of 41 % and 33 %, respectively. The γ spectrum resolutions are 1.86 keV and 1.77 keV at 1.33 MeV of ^{60}Co. The real acquisition times (T_r) ranged from 2 to 4 days. Theoretical details are presented in Duch et al. (2015).

2.3 Cluster analysis of back trajectories

The Hybrid Single-Particle Lagrangian Integrated Trajectory (HYSPLIT) model (version 4; Draxler and Hess, 1998; Draxler et al., 2009) was used to study the main large-scale patterns of air transport to the city of BCN. HYSPLIT was driven with meteorological data from the Global Data Assimilation System (GDAS) reanalysis archive maintained by the Air Resources Laboratory (ARL), which is freely available on-line at http://ready.arl.noaa.gov/. 10.080 kinematic 3D back trajectories were computed twice per day (at noon and midnight) for a period of 14 years (2001-2014). Following Izquierdo et al., 2014, the back trajectories were initialized at 1500 m, which is representative of the mean synoptic transport of the upper boundary layer and the lower troposphere (e.g. Jorba et al., 2004; Izquierdo et al., 2014; Banks et al., 2015), and integrated back in time for 7 days. The length of the back trajectories was selected in relation with the time of collection of the sampled air on the filters, as explained in section 2.2. Although the increasing of the length of the back trajectory also increases the uncertainties associated with it, as the present study does not aim at localizing any particular source but at investigating the main atmospheric circulation patterns over Barcelona, clusters of long term back trajectories were here used. Indeed longer term trajectories are best used in a statistical sense such as "trajectory clustering" to determine transport regimes (e.g. Freitag et al., 2014). In addition, a survey of results from previous studies employing different techniques suggests that average trajectory errors are on the order of 15–20% of the distance travelled after a few days (Stohl, 1998). The final back trajectories were divided into groups by means of a cluster analysis, which is a widely used statistical multivariate technique to explore recurrent patterns within large datasets (Brankov et al., 1998; Cape et al., 2000; Cristofanelli et al., 2006; Liu et al., 2013; Piñero-García et al., 2015). Back trajectories were clustered by minimizing the relative distance of each single trajectory from the trajectories centroids based on the Haversine formula of the great-circle as explained by Jorba et al. (2004).

2.4 Astronomical, meteorological and climate data

Sunspots occur in the Sun's photosphere when temporary darker areas appear compared to surrounding regions. They correspond to a higher concentration of the magnetic field flux that inhibits convection and results in reduced surface T compared to the surrounding photosphere. The flux of GCR is reduced during Sunpots occurrence and so is ^{7}Be which is directly created by the former (e.g. Cannizaro et al., 1995; Al-Azmi et al., 2001; Azahra et al., 2003; Renfro et al., 2013; Hernández-Ceballos et al., 2015). The number of sunspots is modulated with decadal frequency by the 11-year solar sunspot cycle. We use daily data of the number of sunspots from the Sunspot Index and the Long-term Solar Observations data center (SILSO data/image, Royal Observatory of Belgium, Brussels) and correlated them with ^{7}Be concentration on annual basis.

Meteorological data of RH and T for the city of Barcelona were obtained from the Automatic Meteorological Station Net of the Catalan Meteorological Service, and from the Meteorological Equipment Net of the Catalan Government. Monthly means of this previous data were correlated with monthly averages of ^{7}Be and ^{210}Pb concentrations.

The North Atlantic Oscillation (NAO) is one of the main modes of atmospheric variability in the north Atlantic, which is typically characterized by fluctuations in sea level pressure between Iceland and the Azores Islands (e.g. Hurrell, 1995; Hurrel and Desel, 2009). Swings between the positive and negative phases produce large changes in the mean wind speed and direction over the Atlantic, the heat and moisture transport between the Atlantic and the neighboring continents, and the intensity and number of storms, their paths, and their weather (Hurrell et al., 2003). In the Iberian Peninsula, the NAO has been found to influence the precipitation in western and central Spain, while it has a much weaker contribution to the rainfall over the Mediterranean basin of Spain (Rodó et al., 1997; Queralt et al., 2009).

The WeMO is a regional pattern, recently proposed, produced by the sea level pressure difference between southern Spain and northern Italy. WeMO is used to explain the larger fraction of rainfall in this area (Gonzalez-Hidalgo et al., 2009). Indeed, the WeMO index allows the detection of the variability relevant to the cyclogenesis in the far western Mediterranean basin, resulting significantly better than the NAO to explain the monthly pluviometric anomalies during autumn and winter (Martín-Vide and Lopéz-Bustins, 2006).

Monthly data of the NAO and WeMO indexes were used in the present work in relation with the atmospheric concentration of ^{7}Be and ^{210}Pb in Barcelona. NAO data was derived from NOAA (available at https://climatedataguide.ucar.edu/climate-data/hurrell-north-atlantic-oscillation-nao-index-station-based), while the monthly time series of the WeMO index was taken from the Group of Climatology of the University of Barcelona (available at http://www.ub.edu/gc/English/wemo.htm).

3. Results

3.1 Atmospheric variability of ^{7}Be and ^{210}Pb

Seasonal and Inter annual variability under different local meteorological conditions

Figure 1 depicts the weekly time series (in black) of atmospheric concentration of ^{7}Be (upper panel) and ^{210}Pb (bottom panel). The seasonal variability of the time series is presented by means of the 3-month moving average (in green). The ^{7}Be and ^{210}Pb concentrations measured over the whole 14-year period present mean values and corresponding errors of 3.74 ± 0.04 mBq m^{-3} and 0.47 ± 0.01 mBq m^{-3} , respectively. The standard deviations over the dataset are 1.2 mBq m^{-3} and 0.2 mBq m^{-3} for ^{7}Be and ^{210}Pb, respectively.

Figure 2 shows the box plot of the average monthly concentration of ^{7}Be (upper panel), ^{210}Pb (central panel) and their ratio $^{7}Be/^{210}Pb$ (bottom panel) for the whole period. Both radionuclides exhibit a marked seasonality. On the one hand, the concentration of ^{7}Be is minimum in winter, with median values ranging between 2.83 ± 0.03 mBq m^{-3} in December and 2.95 ± 0.04 mBq m^{-3} in January, and maximum in summer, with concentrations between 5.18 ± 0.05 mBq m^{-3} in June and 4.61 ± 0.06 mBq m^{-3} in July. ^{210}Pb largely increases from May (0.42 ± 0.01 mBq m^{-3}) to September (0.63 ± 0.01 mBq m^{-3}). The $^{7}Be/^{210}Pb$ ratio shows a maximum in winter-spring seasons and a minimum in the summer-fall seasons.

Figure 2 highlights a 2-month lag relation between the seasonalities of ^{7}Be and ^{210}Pb. In order to further investigate this relation, the lead-lag correlations between the monthly ^{7}Be and ^{210}Pb time series were calculated. Here we define h as the time lag (in months) between both radionuclides, so that the time series of ^{7}Be is leading the time series of ^{210}Pb when h is negative, and is lagged when h is positive (i.e. ^{7}Be is shifted by h months). Table 1 depicts the lead-lag relation for different values of the lead/lag factor h. Results are in line with the above-mentioned delay between seasonalities, given that correlations are positive for lead times of ^{7}Be from h = -4 to h = +1. Nevertheless, the maximum correlation is found for the simultaneous time series (h = 0). This double behavior, with maximum correlation for h = -2 between the seasonalities and h = 0 for the raw time series, provides some insight into the mechanisms explaining the variability of both radionuclides, both at seasonal and interannual timescales. Thus, the monthly variability of ^{7}Be and ^{210}Pb is largely and simultaneously influenced by a set of common atmospheric factors, while the delay in the seasonalities might reflect differences in the factors modulating the annual cycle (e.g. the radionuclide sources, see the Discussion section).

Figure 3 shows the box plots of the average monthly values of local T (ºC), in the upper panel, and RH (%), in the bottom panel. Median T values range between 9 ºC in winter and 22 ºC in summer. The upper panels of Figures 2 and 3 show a zero-lag relation between the seasonalities of atmospheric ^{7}Be concentrations and the local T measured at the Barcelona station. On the other hand, RH (Figure 3, bottom panel) shows a less pronounced annual cycle and large variability within each month. Median values of RH of around 70% are observed in Barcelona, with lower values during the dry season (summer) and larger values during the rainy season (mainly autumn).

Figure 4 depicts the monthly averages of atmospheric ^{210}Pb (upper-left panel) and ^{7}Be (bottom-left panel) concentrations and T (upper-right panel) and RH (bottom-right panel) conditions for each year. These plots show some major outliers (coloured rings) in ^{7}Be and ^{210}Pb (left panels) that cannot be explained neither by the seasonal variability of the radionuclides nor by the local meteorological conditions. Indeed, when these plots are compared with Figure 4, and taking into account only some of the major outliers, we observe that:

1. June and August 2003: they show high concentration values for ^{210}Pb (green circle) but not for ^{7}Be. These months corresponded to extremely high T and to low RH values;
2. July 2006: the highest values of both ^{210}Pb and ^{7}Be were recorded, together with the highest T values and the lowest RH conditions over the whole year;
3. September and October 2008: they correspond to the highest values of ^{210}Pb and ^{7}Be over the year, but in this case, this did not correspond to extreme T and RH conditions;
4. March and April 2012: only high ^{7}Be concentration values and low RH were reported;
5. July 2013: it corresponded to the highest values of both ^{210}Pb and ^{7}Be and the driest RH conditions over the year;
6. The smallest values of ^{7}Be were observed in January 2001, 2004 and 2006 and in February 2005. The lowest T over the year was observed for the latter case, but no large anomaly was found for the others events.

Inter annual variability related to sun spots cycle

Figure 5 shows the year-to-year variability of annual mean ^{7}Be (black circles), ^{210}Pb (red circles) and the number of sun spots (blue circles). The variability of the annual mean solar activity is seen to be negatively correlated with the atmospheric concentration of ^{7}Be. Instead, the annual time series of ^{210}Pb variability is not influenced by the solar activity. We note that a decreasing trend of 20% was observed for ^{210}Pb over the 14-year period.

3.2 Origin of air masses and role of climate

Following the methodology of Izquierdo et al., 2014, the main pathways of air masses arriving at the sampling station have been described by means of back trajectories in a particle trajectory model. Atmospheric values of ^{7}Be and ^{210}Pb were associated with the back trajectories in order to infer the areas and sources of high and low radionuclide concentrations. The analysis was performed by considering those cases with concentrations below the 25th percentile and above the 75th percentile, which correspond to 2.8 mBq m^{-3} and 4.5 mBq m^{-3} for ^{7}Be (left panels) and 0.3 mBq m^{-3} and 0.6 mBq m^{-3} for ^{210}Pb (right panels).

High concentrations of ^{7}Be and ^{210}Pb (Figure 6, upper panels) are mainly associated with back trajectories passing with larger frequency (violet regions) over land and mainly over the north of Spain and the south of France, in correspondence to the Catalan Pyrenees. Low ^{7}Be and ^{210}Pb concentrations (Figure 6, bottom panels) are related with air masses with more disperse footprints and passing more frequently over northwestern Atlantic Ocean (violet regions). A comparison between the footprints associated with high and low radionuclides concentrations show that: i) low concentrations are related with air masses coming from the north-west of the city (10-25%, red regions), while ii) high concentrations are also associated with air masses coming from the south (10-25%, red regions). Figure 6 also shows that long-range air masses usually come from the WNW direction (red area), passing over these previous areas with a frequency between 10-25 % (see the Discussion section).

A cluster analysis was applied to the back trajectories to define the main long range patterns of air transport to the city of Barcelona. In agreement with Jorba et al (2004) and Banks et al. (2015), the main six groups identified in this analysis are the Atlantic Occidental Slow (C1_AOS), North Atlantic Medium (C2_NAM), North Atlantic Slow (C3_NAS), North Atlantic Fast (C4_NAF), Regional (C5_R) and European (C6_E) clusters:

- C1_AOS (21% of cases) is a short range cluster with origin over the Atlantic Ocean and arriving at Barcelona after travelling 90% of the time over the ocean;
- C2_NAM (17%) is a medium range cluster arriving at Barcelona from the eastern coast of Canada and spending 80% of its time over the ocean;
- C3_NAS (16%) is a short range cluster with origin over the North Atlantic region and spending 90% of its time over the ocean;
- C4_NAF (7%) is a long range cluster arriving in Spain from the west. Baeza et al. (2012) showed evidences of artificial radionuclides released from the Fukushima Dai-ichi nuclear power station and transported to Barcelona by these long range air masses;
- C5_R (20%) is a short range cluster characterized by weak winds and high residence times over Spain;
- C6_E (19%) is an European short range cluster arriving at Barcelona from the east.

The variability of the concentrations of ^{7}Be and ^{210}Pb was analysed with regard to each cluster and the associated average height of their origin (Figure 7). In addition, the variability of the monthly NAO and the WeMO indexes and of the monthly local T and RH conditions, measured at Barcelona, was also calculated in relation with the previous back trajectory clusters (Figure 7). The boxplots in Figure 7a-h show for each cluster the average values of ^{7}Be, ^{7}Be/^{210}Pb, ^{210}Pb, origin height, NAO, T, WeMO and RH, respectively.

Panels 7a-d show that air masses from clusters C6_E and C5_R correspond to the largest values of ^{210}Pb and ^{7}Be, as well as to the lowest values of ^{7}Be/^{210}Pb and of the altitude of the back trajectories. The NAO index (Figure 7e) shows highest value, and with less variability, when air masses come to Barcelona within the the C4_NAF cluster. In addition, the value of the NAO index is smallest in the C3_NAS cluster, although the associated uncertainty range is also the largest. Regarding the WeMO index, differences between clusters are smaller, although the smallest variability of the index is observed under the clusters C3_NAS and C4_NAF (Figure 7g). In addition, the WeMo index is slightly larger in the clusters C1_AOS, C5_R and C6_E. The highest T values are observed in the cluster C5_R and the lowest values in the cluster C4_NAF (Figure 7f). No significant differences are observed in RH among clusters (Figure 7g), although values are slightly larger in the cluster C4_NAF.

Table 2 shows the mean values and the standard errors of ^{7}Be and ^{210}Pb for each cluster. A t-test analysis was performed to analyze the differences of ^{7}Be and ^{210}Pb between each couple of clusters, and it indicates that there is no significant difference ($p < 0.05$) between the clusters C1_AOS, C2_NAM, C3_NAS and C4_NAF. However, average concentrations in clusters C5_R and C6_E are significantly different with regard to both radionuclides.

Table 2 also shows, for each cluster of back trajectories, the Spearman correlations between the monthly values of ^{7}Be and ^{210}Pb with the monthly time series of the NAO and WeMO indexes, T and RH. A perfect Spearman correlation of +1 (−1) occurs when there is a monotonically increasing (decreasing) correspondence between the values of the variables. None of the correlations with the NAO index have been found to be statistically significant at the 5% level. Significant negative correlations were instead found between the WeMO index and ^{7}Be and ^{210}Pb in the C1_AOS, C2_NAM, C3_NAS and C6_E clusters. In this way, the WeMO index seems to better represent the variability of the radionuclides over the eastern region of Spain. Positive correlations have been found between both ^{7}Be and ^{210}Pb concentrations and the local T in almost all clusters. In contrast, negative correlations have been found between ^{7}Be and the observed RH. No significant correlations were found between ^{210}Pb and local relative humidity (see the Discussion section).

4. Discussion

The mean atmospheric ^{7}Be concentration over the period 2001-2014 is found to be in general agreement with previous studies, after taking into account the dependency between the radionuclide concentrations and latitude of the sampling site (e.g. Kulan et al., 2006; Leppanen et al., 2012; Hernández-Ceballos et al., 2015). Moreover, in line with previous results (e.g. Todorovic et al., 2005; Dueñas et al., 2009; Tositti et al., 2014; Gordo et al., 2015) our results show a positive correlation between monthly measurements of ^{210}Pb and ^{7}Be.

Figures 2 and 3 showed the box plots of ^{7}Be and ^{210}Pb, T and RH measured in Barcelona between 2001 and 2014. Taking into account that both radionuclides are simultaneously measured under the same atmospheric conditions, the difference in the seasonal variability of their concentrations must be the result of the different seasonality and strength of their respective sources and sinks.

Increases in the cosmogenic ^{7}Be concentrations, observed simultaneously with the seasonal increase of temperatures, could be associated with the intensification of the solar irradiance, which contributes to the atmospheric warming and the subsequent vertical mixing between the upper and lower layers of the troposphere. In this way, the tropospheric ^{7}Be could be easily transported down to the surface layer. The terrestrial ^{210}Pb depends on the release of ^{222}Rn in the atmosphere, which is usually highest during the warm season (Grossi et al., 2011; López-Coto et al., 2013; Vargas et al., 2015) and can be accumulated during the night within the shallow atmospheric surface layer, leading to an increase in the total weekly ^{210}Pb concentrations before it escapes to the higher troposphere. Differences in the timing of these two mechanisms could explain the 2-month lag between the seasonalities of ^{7}Be and ^{210}Pb. We note that this delay was also observed in Tositti et al., 2014.

Figure 4 was used to identify some of the major monthly outliers in ^{7}Be and ^{210}Pb that cannot be simply explained by means of the local T and RH conditions or the seasonal variability of the atmospheric concentration of the radionuclides. Particularly, the event occurred in summer 2003 coincides with an unprecedented record-breaking heat wave that affected western Europe (Beniston and Diaz, 2004) and the city of Barcelona (Borrell et al. 2006, Ballester et al. 2011). The observed ^{210}Pb increase could be related with a strong increase of ^{210}Pb within the lower atmosphere, due to ^{222}Rn exhaled from local sources under high T and low RH conditions associated with heat waves and facilitating the ^{222}Rn exhalation form the soil (e.g. Grossi et al., 2011; López-Coto et al., 2013, Karstens et al., 2015). The lack of a corresponding increase in ^{7}Be could be explained by the low sun activity during this year. Stefanon et al. (2012) showed that another intense European heat wave event was recorded in July 2006 in certain European countries. A close inspection to Figure 4 shows that in this case both radionuclides exhibited highest concentrations in July of that year, together with warm and dry conditions over the year. Regarding these episodes, Weigel et al. (2012) detected also an event of stratospheric intrusion near the subtropical jet over the Mediterranean Sea during a flight campaign on July 29th 2006, which could explain the observed increase in the ^{7}Be concentration during this episode. 2006 was also a year with high production of cosmogenic ^{7}Be due to the sun activity. High values of monthly ^{210}Pb and ^{7}Be were observed in September and October 2008, which could not be explained by extreme T and RH conditions. The analysis of data reveals that during the week between 17th and 24th of September 2008, high concentrations of both radionuclides were observed in Barcelona (8.52 ± 0.13 mBq m^{-3} for ^{7}Be and 1.29 ± 0.18 mBq m^{-3} for ^{210}Pb). The cluster analysis shows that the associated back trajectory cluster during this event was C5_R. In the first and third weeks of October 2008, measured concentrations of

^{7}Be and ^{210}Pb were 6.97 ± 0.18 mBq m^{-3} and 1.20 ± 0.15 mBq m^{-3}, respectively. These values were associated with the C4_NAF and C5_R clusters. This example confirms the observed increase in both radionuclide concentrations when westerly air masses are coming from the Iberian Peninsula through the low atmospheric layer. ^{7}Be concentrations were largest in July 2006 and 2013, and in March/April 2012, with dry atmospheric conditions. Trickl et al. (2015) described episodes of stratospheric intrusion in July 2013 with large-scale transport of smoke from fires in the North of America and eastern Siberia to the Alps in Europe (e.g. Cristofanellli et al., 2006; Lee et al., 2007). Although a deep analysis of heat wave and stratospheric intrusion events is out of the scope of this work, simultaneous measurements of ^{7}Be and ^{210}Pb can be an useful tool for the study of this type of events.

Figure 6 presents the frequency distribution map of air masses arriving at Barcelona when low or high concentrations of ^{7}Be (left panels) and ^{210}Pb (right panels) are observed. Radionuclide concentrations increase when air masses spend most of the time over land. In the particular case of ^{210}Pb, this could be due to the atmospheric uptake of the exhaled ^{222}Rn and its subsequent decay. The increase in the ^{7}Be concentrations could be due to the increase of atmospheric vertical mixing over the Pyrenees, as already described in the Alps by other authors. However this hypothesis cannot be tested because the weekly temporal resolution of our data does not allow a deeper analysis of these events. On the other side, humid air masses with large residence times near water surfaces, such as the Atlantic Ocean, had less ^{210}Pb uptake, due to negligible ^{222}Rn exhalation from water bodies, and much more uptake of water vapour that could facilitate the washout of both ^{210}Pb and ^{7}Be radionuclides.

Figure 7 and Table 2 show a significant increase in the concentrations of ^{7}Be and ^{210}Pb within the regional and European clusters. These clusters, which occur with a total frequency of 39 %, also exhibit the lowest height in their origin. The concentration of ^{7}Be could increase due to its transport from higher European latitudes (45º-60º), which usually present larger atmospheric ^{7}Be concentrations (e.g. Leppanen et al., 2012; Hernández-Ceballos et al., 2015). The increase of ^{210}Pb could be explained by its uptake by the air masses travelling to Barcelona. In addition, results show that the WeMO index, in comparison with the NAO index, seems to better represent the variability of the radionuclides over the northeastern region of Spain. This result is in agreement with Martín-Vide et al., 2006 and Izquierdo et al., 2014, for air pollutants and rainfall intensity variability in this area. In fact, a negative phase of the WeMO index is generally associated with weakened northerly winds, which can increase the atmospheric concentrations of ^{7}Be and ^{210}Pb in Barcelona. The positive phase of the WeMO indicates the occurrence of enhanced westerlies and northerlies from the Atlantic Ocean, and these air masses have been associated with a decrease of atmospheric radionuclide concentrations measured in Barcelona. ^{7}Be concentrations in almost each cluster have been strongly linked to the local T and RH conditions. Indeed, high temperatures favour the atmospheric vertical mixing and lead to the intrusion of dry stratospheric air masses that are rich in ^{7}Be within the surface layer.

5. Conclusions

In the present study, we performed an in-depth analysis of the variability of atmospheric ^{7}Be and ^{210}Pb concentrations in the city of Barcelona for the period 2001-2014 by using different tools, such as local meteorological parameters, regional and global climate indexes and a clusters analysis of model back trajectories of atmospheric transport. The main aim of this work was to address the seasonal and inter-annual variability of the atmospheric concentrations of two radionuclides characterized by different sources and measured under the same atmospheric conditions.

Results show a strong correlation between both ^{7}Be and ^{210}Pb with local T variability, which can favour the STE and the ^{222}Rn exhalation from the ground. In addition, regional and European air masses are found to transport atmospheric ^{7}Be and ^{210}Pb to the city of Barcelona. Finally, for the first time, the variability of the regional WeMo index was found to be linked to the radionuclide concentrations. This analysis shows that this index, defined as the difference in atmospheric pressure between two sites across the western Mediterranean Sea, can explain better the radionuclide variability in northwestern Spain than the NAO index.

Although the weekly resolution of the measured ^{210}Pb and ^{7}Be data is not enough to statistically quantify the heat wave and stratospheric intrusion events influencing the radionuclide concentrations, our study confirms that simultaneous measurements of ^{7}Be, ^{210}Pb and local meteorological parameters could be potentially useful to identify and differentiate this type of episodes. However, in order to investigate more in depth the application of this tool for the diagnostic of these events over a larger European area, we will need to include in future studies harmonized datasets of atmospheric ^{7}Be and ^{210}Pb measured at different European stations.

Acknowledgments

This work has been supported by: the Nuclear Safety Council (CSN) within the framework of the Environmental Radiological Surveillance Program which operates in Spain under its control and responsibility, the Obra Social "La Caixa" (www.obrasocial.lacaixa.es) with the ClimaDat Project (www.climadat.es) and the Ministerio Español de Economia y Competividad funding the MIP project (Methane interchange between soil and air over the Iberian península reference: CGL2013-46186-R).

CG particularly thanks the Ministerio Español de Educación, Cultura y Deporte to partially support her work with the research mobility grant "Josè Castillejos" (ref. CAS15/00042). CG also thanks Dr. Delia Arnold for the nice discussions about atmospheric transport models applications and back trajectories consistency.

JB gratefully acknowledges funding from the European Commission through a Marie Curie International Outgoing Fellowship (project MEMENTO from the FP7-PEOPLE-2011-IOF call) and from the European Commission and the Catalan Government through a Marie Curie - Beatriu de Pinós Fellowship (project 00068 from the BP-DGR-2014-B call).

Authors also thank: the University Corporation for Atmospheric Research (UCAR) for NAO data (climatedataguide.ucar.edu/climate-data/hurrell-north-atlantic-oscillation-nao-index-station-based); the University of Barcelona for WeMO data (www.ub.edu/gc/English/wemo.htm); the Sunspot Index and Long-term Solar Observations data center for sunspots numbers data (www.sidc.be/silso/datafiles); David Carslaw and Karl Ropkins, developers of the R package OpenAir (www.openair-project.org), and Richard Iannone, developer of the R package SplitR (github.com/rich-iannone/SplitR), both used in the present work for data analysis.

Meteorological data were available thank to the "Xarxa d'Estacions Meteorològiques Automàtiques (XEMA)" of the "Servei Meteorològic de Catalunya (SMC)", integrated within the "Xarxa d'Equipaments Meteorològics de la Generalitat de Catalunya (Xemec)" (meteo.cat/observacions/xema/dades?codi=D5).

Authors are really grateful to the comments and suggestions of the three reviewers which strongly helped the improvement of our manuscript.

References

Aldahan, A., Possnert, G., Vintersved, I., 2001. Atmospheric interactions at northern high-latitudes from weekly Be-isotopes in surface air. Appl. Radiat. Isotop. 54, 345–353, doi: 10.1016/s0969-8043(00)00163-9.

Azahra, M., Camacho-García, A., González-Gómez, C., López-Penalver, J., El Bardouni, T., 2003. Seasonal ^{7}Be concentrations in near-surface air of Granada (Spain) in the period 1993–2001. Appl. Radiat. Isotop. 59, 159–164, doi: 10.1016/s0969-8043(03)00154-4

Al-Azmi, D., Sayed, A.M., Yatim, H.A., 2001. Variations in ^{7}Be concentrations in the atmosphere of Kuwait during period 1994 to 1998. Appl. Radiat. Isotop. 55, 413–417, doi: 10.1016/s0969-8043(01)00077-x.

Baeza, A., Corbacho, J.A., Rodríguez, A., Galván, J., García-Tenorio, R., Manjón, G., Mantero, J., Vioque, I., Arnold, D., Grossi, C., Serrano, I., Vallés, I., Vargas, A., 2012. Influence of the Fukushima Dai-ichi nuclear accident on Spanish environmental radioactivity levels. J. of Environ. Radioact. 114 (A), 138-143, 10.1016/j.jenvrad.2012.03.001.

Ballester, J., Robine, J.M., Herrmann, F.R., Rodó, X., 2011. Long-term projections and acclimatization scenarios of temperature-related mortality in Europe. Nature Communications 2, 358, doi: 10.1038/ncomms1360.

Banks, R.F., Tiana-Alsina, J., Rocadenbosch, F., Baldasano, J.M., 2015. Performance Evaluation of the Boundary-Layer Height from Lidar and the Weather Research and Forecasting Model at an Urban Coastal Site in the North-East Iberian Peninsula. Boundary-Layer Meteorol., 157-265, doi:10.1007/s10546-015-0056-2.

Baskaran, M., Coleman, C. H., Santschi, P.H., 1993. Atmospheric deposition fluxes of ^{7}Be and ^{210}Pb at Galveston and College Station, Texas. J. of Geophys. Res. 98, 20555–20571, doi: 10.1029/93jd02182.

Baskaran, M., 2011. Po-210 and Pb-210 as atmospheric tracers and global atmospheric Pb-210 fallout: a Review. J. of Environ. Radioact. 102, 500-513, doi: 10.1016/j.jenvrad.2010.10.007.

Beniston, M., Diaz, H. F., 2004. The 2003 heat wave as an example of summers in a greenhouse climate? Observations and climate model simulations for Basel, Switzerland. Global and Planetary Change 44, 1–4, 73–81, doi: 10.1016/j.gloplacha.2004.06.006.

Bonotto, D. M., and Vergotti, M., 2015. ^{210}Pb and compositional data of sediments from Rondonian lakes, Madeira River basin, Brazil. Appl. Radiat. Isotop. 99, 5–19, doi: 10.1016/j.apradiso.2015.02.002.

Borrell, C., Marí-Dell'Olmo, M., Rodríguez-Sanz, M., Garcia-Olalla, P., Cayla, J.A., Benach, J., Muntaner, C., 2006. Socioeconomic position and excess mortality during the heat wave of 2003 in Barcelona. European J. of Epidemiology 21, 633-640, doi: 10.1007/s10654-006-9047-4.

Brankov, E., Rao, S.T., and Porter, P.S., 1998. A Trajectory-Clustering-Correlation Methodology for Examining the Long-Range Transport of Air Pollutants. Atmos. Environ. 32, 1525-1534, doi: 10.1016/s1352-2310(97)00388-9.

Cannizaro, F., Greco, G., Raneli, M., Spitale, C., Tomarchio, E., 1995. Behavior of ^{7}Be air concentrations observed during a period of13 years and comparison with sun activity. Nucl. Geophys. 9, 597–607.

Cape, J. N., Methven, J. and Hudson, L. E., 2000. The use of trajectory cluster analysis to interpret trace gas measurements at Mace Head, Ireland. Atmos. Environ. 34, 3651-3663, doi: 10.1016/s1352-2310(00)00098-4.

Cristofanelli, P., Bonasoni, P., Tositti, L., Bonafè, U., Calzolari, F., Evangelisti, F., Sandrini, S., Stohl, A. 2006. A 6-years analysis of stratospheric intrusions and their influence on ozone at Mt. Cimone (2165 m above sea level). J. of Geophys. Res. 111, D03306, doi:10.1029/2005JD006553.

Dall'Osto, M., Querol, X., Alastuey, A., Minguillon, M.C., Alier, M., Amato, F., Brines, M., Cusack, M., Grimalt, J.O., Karanasiou, A., Moreno, T., Pandolfi, M., Pey, J., Reche, C., Ripoll, A., Tauler, R., Van Drooge, B.L., Viana, M., Harrison, R.M., Gietl, J., Beddows, D., Bloss, W., O'Dowd, C., Ceburnis, D., Martucci, G. N. L., Worsnop, D., Wenger, J., Mc Gillicuddy, E., Sodeau, J., Healy, R., Lucarelli, F., Nava, S., Jimenez, J.L., Gomez Moreno, F., Artinano, B., Prévôt, A.S.H., Pfaffenberger, L., Frey, S., Wilsenack, F., Casabona, D., Jiménez-Guerrero, P., Gross, D., Cots, N., 2013. Presenting SAPUSS: Solving Aerosol Problem by Using Synergistic Strategies in Barcelona, Spain. Atmos. Chem. Phys., 13, 8991-9019, doi:10.5194/acp-13-8991-2013.

Dorman, L., 2004. Cosmic Rays in the Earth's Atmosphere and Underground. Kluwer Acad., Dordrecht, Netherlands, doi: 10.1007/978-1-4020-2113-8_2.

Draxler, R.R., and G.D. Hess, 1998. An overview of the HYSPLIT_4 modeling system of trajectories, dispersion and deposition. Aust. Meteor. Mag. 47, 295-308**.**

Draxler, R.R., Stunder, B., Rolph, G., Taylor, A. 2009. HYSPLIT_4 User's Guide, via NOAA ARL website. NOAA Air Resources Laboratory, Silver Spring, MD, December 1997.

Duch, M.A., Serrano, I., Cabello, V., Camacho, A., 2015. Comparison of different sampling methods for the determination of low-level radionuclides in air. Appl. Radiat. Isotop. 109, 456-459, di: 10.1016/j.apradiso.2015.11.042.

Dueñas, C., Fernández, M.C., Cañete, S., Pérez, M., 2009.^{7}Be to ^{210}Pb concentration ratio in ground level air in Málaga (36.7°N, 4.5°W). Atmos. Res. 92, 49–57, doi: 10.1007/978-1-4020-6475-3_156.

Feely, H.W., Larsen, R.J., Sanderson, C.G., 1989. Factors that cause seasonal variations in beryllium-7 concentrations in surface air. J. of Environ. Radioact. 9, 223–249, doi: 10.1016/0265-931x(89)90046-5.

Forbush, S., 1954. World-wide cosmic-ray variations, 1937–1952. J. of Geophys. Res. 59 (4), 525–542, doi: 10.1029/sp037p0183.

Freitag, S., Clarke, A.D., Howell, S.G., Kapustin, V.N., Campos, T., Brekhovskikh, V.L., Zhou, J. 2014. Combining airborne gas and aerosol measurements with HYSPLIT: a visualization tool for simultaneous evaluation of air mass history and back trajectory consistency. Atmos. Meas. Tech., 7, 107–128, doi: :10.5194/amt-7-107-2014.

Galmarini, S., and Thunis, P., 1999. On the validity of Reynolds assumptions for running-mean filters in the absence of a spectral gap. J. Atmos. Sci., 57, 2968-2976, doi: 10.1175/1520-0469(1999)056<1785:otvora>2.0.co;2 .

Galmarini, S., Michelutti, F., and Thunis, P., 2000. Estimating the contribution of Leonard and cross terms to the subfilter from atmospheric measurements. J. Armos. Sci., 57, 2968-2976, doi: 10.1175/1520-0469(2000)057<2968:etcola>2.0.co;2 .

Gonzalez-Hidalgo, J.C., Lopez-Bustins, J.A., Stepánek, P., Martin-Vide, J., de Luis, M., 2009. Monthly precipitation trends on the Mediterranean fringe of the Iberian Peninsula during the second-half of the twentieth century (1951-2000). International Journal of Climatology 29, 1415-1429, doi: 10.1002/joc.1780.

Gordo , E., Liger , E., Duenas, C., Fernandez, M.C., Canete, S., Perez, M., 2015. Study of ^{7}Be and ^{210}Pb as radiotracers of African intrusions in Malaga (Spain). J. of Environ. Radioact. 148, 141-153, doi: 10.1016/j.jenvrad.2015.06.028.

Grossi, C., Vargas, A., Camacho, A., López-Coto, I., Bolívar, J.P., Xia, Y., Conen, F., 2011. Inter-comparison of different direct and indirect methods to determine radon flux from soil, Radiat. Meas., 46(1), 112-118, doi: 10.1016/j.radmeas.2010.07.021.

Hernández-Ceballos, M.A., Adame, J.A., Bolívar, J.P., de la Morena, B.A., 2013. Vertical behaviour and meteorological properties of air masses in the southwest of the Iberian Peninsula (1997-2007). Meteorol. Atmos. Phys. 119, 163-175, doi: 10.1007/s00703-012-0225-5.

Hernández-Ceballos, M. A., Cinelli, G., Marín Ferrer, M., Tollefsen, T., De Felice, L., Nweke, E., Tognoli, P.V., Vanzo, S., De Cort, M., 2015. A climatology of ^{7}Be in surface air in European Union. J. of Environ. Radioact. 141, 62-70, doi: 10.1016/j.jenvrad.2014.12.003.

Hurrell, J.W., 1995. Decadal trend in the North-Atlantic oscillation e regional temperatures and precipitation. Science 269, 676-679, doi: 10.1126/science.269.5224.676.

Hurrell, J.W. and C. Deser, 2009. North Atlantic climate variability: the role of the North Atlantic Oscillation. J. Mar. Syst., 78 (1), 28-41, doi: 10.1016/j.jmarsys.2008.11.026.

Hurrell, J.W., Kushnir, Y., Ottersen, G., Visbeck, M., 2003. An Overview of the North Atlantic Oscillation. The North Atlantic Oscillation: Climatic Significance and Environmental Impact. Geophysical Monograph 134, doi: 10.1029/2003eo080005.

Izquierdo, R., Alarcón, M., Aguillaume, L., Àvila, A., 2014. Effects of teleconnection patterns on the atmospheric routes, precipitation and deposition amounts in the north-eastern Iberian Peninsula. Atmos. Environ. 89, 482-490, doi: 10.1016/j.atmosenv.2014.02.057.

Jacobi, W., 1963. Die Natürliche Radioaktivität der Atmosphäre. Biophysik 1, 175–188.

Johnson, W., Viezee, W., 1981. Stratospheric ozone in the lower troposphere: Presentation and interpretation of aircraft measurements. Atmos. Environ. 15, 1309–1323, doi: 10.1016/0004-6981(81)90325-5.

Jorba, O., Perez, C., Rocadenbosch, F., and Baldasano, J., 2004. Cluster Analysis of 4-Day Back Trajectories Arriving in the Barcelona Area (Spain) from 1997 to 2002. J. Appl. Meteorol., 43 887–901, doi: 10.1175/1520-0450(2004)043<0887:caodbt>2.0.co;2.

Karstens, U., Schwingshackl, C., Schmithüsen, D., Levin, I., 2015. A process-based ^{222}Radon flux map for Europe and its validation by long-term observations, Atmos. Chem. Phys. Discuss. 15, 17397–17448, doi: 10.5194/acpd-15-17397-2015.

Kikuchi, S., Sakurai, H., Gunji, S., Tokanai, F., 2009. Temporal variation of ^{7}Be concentrations in atmosphere for 8y from 2000 at Yamagata, Japan: solar influence on the ^{7}Be time series. J. of Environ. Radioact. 100, 515–521, doi: 10.1016/j.jenvrad.2009.03.017.

Kirpa, R., and Sarin, M.M., 2012. Atmospheric ^{210}Pb, ^{210}Po and ^{210}Po/^{210}Pb activity ratio in urban aerosols: temporal variability and impact of biomass burning emission. Tellus B, 1-11, doi: 10.3402/tellusb.v64i0.17513.

Kottek, M., Grieser, J., Beck, C., Rudolf, B., Rubel, F., 2006. World Map of the Köppen–Geiger climate classification updated. Meteorol. Z. 15 (3), 259–263, doi: 10.1127/0941-2948/2006/0130.

Kulan, A., Aldahan, A., Possnert, G., Vintersved, I. 2006. Distribution of ^{7}Be in surface air of Europe. Atmos. Environ. 40, 3855–3868, doi: 10.1016/j.atmosenv.2006.02.030.

Lee, H. N., Tositti, L., Zheng, X., Bonasoni, P., 2007. Analyses and comparisons of variations of ^{7}Be, ^{210}Pb, and ^{7}Be/^{210}Pb with ozone observations at two Global Atmosphere Watch stations from high mountains. J. of Geophys. Res. 112, D05303, di: 10.1029/2006jd007421.

Lee, H.-I., Huh, C.-A., Lee, T., Huang, N.E., 2015.Time series study of a 17-year record of ^{7}Be and ^{210}Pb fluxes in northern Taiwan using ensemble empirical mode decomposition. J. of Environ. Radioact. 147, 14-21, doi: 10.1016/j.jenvrad.2015.04.017.

Leppanen, A.-P. Pacini, A.A., Usoskin, I.G., Aldahan, A., Echer, E., Evangelista, H., Klemola, S., Kovaltsov, G.A., Mursula, K., Possnerti, G., 2010. Cosmogenic ^{7}Be in air: A complex mixture of production and transport. J. of Atmos. and Solar-Terrestrial Phys. 72, 1036–1043, doi: 10.1016/j.jastp.2010.06.006.

Leppanen, A.-P., Usoskin, I.G., Kovaltsov, G.A., Paatero, J., 2012. Cosmogenic ^{7}Be and ^{22}Na in Finland: Production, observed periodicities and the connection to climatic phenomena. J. of Atmos. and Solar-Terrestrial Phys. 74, 164–180, doi: 10.1016/j.jastp.2011.10.017.

Liu, N., Yu Ye, He, J., Zhao, S., 2013. Integrated modeling of urban–scale pollutant transport: application in a semi–arid urban valley, Northwestern China. Atm. Pol. Res. 4, 306-314, doi: 10.5094/apr.2013.034.

López-Coto, I., Mas, J.L., Bolivar, J.P., 2013. A 40-year retrospective European radon flux inventory including climatological variability. Atmos. Environ. 73, 22–33, doi: 10.1016/j.atmosenv.2013.02.043.

Martín-Vide, J., Lopez-Bustins, J.A., 2006. The Western Mediterranean Oscillation and rainfall in the Iberian Peninsula. International J. of Climatology 26, 1455-1475, doi: 10.1002/joc.1388.

Meehl, G.A., van Loon, H., 1979. The seesaw in winter temperatures between Greenland and northern Europe. Part III: teleconnections with lower latitudes. Mon Weather Rev 107, 1095-1106, doi: 10.1175/1520-0493(1979)107<1095:tsiwtb>2.0.co;2.

Millan, M.M., Salvador, R., Mantilla, E., Kallos, G., 1997. Photooxidant dynamics in the Mediterranean Basin in summer: results from European research projects. J. Geophys. Res., 102, 8811– 8823, doi: 10.1029/96JD03610.

Papastefanou, C., Ioannidou, A., 1995. Aerodynamic size association of Be-7 in ambient aerosols. J. Environ. Radioact. 26, 273–282, doi: 10.1016/0265-931x(94)00011-k.

Piliposian, G.T. and Appleby, P.G. 2003. A simple model of the origin and transport of ^{222}Rn and ^{210}Pb in the atmosphere. Continuum Mechanics and Thermodynamics 15 (5), 503-518, doi: 10.1007/s00161-003-0129-1.

Piñero-García, F., Ferro-García, M.A., Chham, E., Cobos-Díaz, M., González-Rodelas, P. 2015. A cluster analsysis of back trajectories to study the behavior of radioactive aerosols in the south-west of Spain. J. of Environ. Radioact. 147, 142-152, doi: 10.1016/j.jenvrad.2015.05.029.

Porstendorfer, J., 1994. Proprieties and behavior of radon and thoron and their decay products in air. J. Aerosol. Sci. 25, 219-263, doi: 10.1016/0021-8502(94)90077-9.

Queralt, S., Hernández, E., Barriopedro, D., Gallego, D., Ribera, P., Casanova, C., 2009. North Atlantic Oscillation influence and weather types associated with winter total and extreme precipitation events in Spain. Atmos. Res. 94, 675–683, doi: 10.1016/j.atmosres.2009.09.005.

Reiter, R., 1991. On the mean daily and seasonal variations of the vertical ozone profiles in the lower troposphere. Atmos. Environ. 25A, 1751-1757, doi: 10.1016/0960-1686(91)90259-a.

Renfro, A.A., Kirk Cochran, J., Colle, B.A., 2013. Atmospheric fluxes of ^{7}Be and ^{210}Pb on monthly time-scales and during rainfall events at Stony Brook, New York (USA). J. of Environ. Radioact. 116, 114-123, doi: 10.1016/j.jenvrad.2012.09.007.

Rodó, X., Baert, E. and Comín, F.A., 1997. Variations in seasonal rainfall in Southern Europe during the present century: relationships with the North Atlantic Oscillation and the El Niño-Southern Oscillation. Climate Dynamics 13: 278-284, doi: 10.1007/s003820050165.

Rodríguez, S., Querol, X., Alastuey, A., Mantilla, E., 2002. Origin of high summer PM10 and TSP concentrations at rural sites in Eastern Spain. Atmos. Environ., 36, 3101–3112, doi: 10.1016/s1352-2310(02)00256-x.

Soriano, C., Baldasano, J. M., Buttler, W. T., Moore, K., 2001. Circulatory patterns of air pollutants within the Barcelona Air Basin in a summertime situation: lidar and numerical approaches. Bound.-Lay. Meteorol., 98, 33–55, doi: 10.1016/j.atmosenv.2004.04.010.

Stefanon, M., D'Andrea, F., Drobinski, P., 2012. Heatwave classification over Europe and the Mediterranean region. Environ. Res. Lett. 7, 14-23, doi: 10.1088/1748-9326/7/1/014023.

Stohl, A. 1998. Computation, accuracy and applications of trajectories- a review and bibliography. Atmos. Environ. 32, 6, 947-966, doi: S1352–2310(97)00457–3.

Stohl, A., Spichtinger-Rakowsky, N., Bonasoni, P., Feldmann, H., Memmesheimer, M., Scheel, H.E., Trickl, T., HuKbener, S., Ringer, W., Mandl, M., 2000. The influence of stratospheric intrusions on alpine ozone concentrations. Atmos. Environ. 34, 1323-1354, doi: 10.1016/s1352-2310(99)00320-9.

Todorovic, D., Popovic, D., Djuric, G., Radenkovic, M., 2005. ^{7}Be to ^{210}Pb concentration ratio in ground level air in Belgrade area. J. of Environ. Radioact. 79, 297–307, doi: 10.1016/j.jenvrad.2004.08.003.

Tositti, L., Brattich, E., Cinelli, G., Baldacci, D. 2014. 12 years of ^{7}Be and ^{210}Pb in Mt. Cimone, and their correlation with meteorological parameters. Atmos. Environ. 87, 108–122, doi: 10.1016/j.atmosenv.2014.01.014.

Trickl, T., Vogelmann, H., Flentje, H., Ries, L., 2015. Stratospheric ozone in boreal fire plumes – the 2013 smoke season over central Europe. Atmos. Chem. Phys., 15, 9631–9649, doi: 10.5194/acp-15-9631-2015.

Usoskin, I., Kovaltsov, G., 2008. Production of cosmogenic ^{7}Be isotope in the atmosphere: full 3D modelling. J. of Geophys. Res. 113, D12107, doi: 10.1029/2007jd009725.

Valles, I., Camacho, A., Ortega, X., Serrano, I., Blazquez, S., 2009. Natural and anthropogenic radionuclides in airborne particulate samples collected in Barcelona (Spain). J. of Environ. Radioact. 100, 102–107, doi: 10.1016/j.jenvrad.2008.10.009.

Vargas, A., Arnold, D., Adame, J.A., Grossi, C., Hernández-Ceballos, M.A., Bolívar, J.P., 2015. Analysis of the vertical radon structure at the Spanish "El Arenosillo" tower station, J. Environ. Radioact., 139, 1-17, doi: 10.1016/j.jenvrad.2014.09.018.

Vecchi, R., Valli, G., 1997. ^{7}Be in surface air: a natural atmospheric tracer. J. Aerosol Sci. 28 (5), 895–900, doi: 10.1016/s0021-8502(97)88763-0.

Weigel, K., Hoffmann, L., Gunther, G., Khosrawi , F., Olschewski, F., Preusse, P., Spang, R., Stroh, F., Riese, M., 2012. A stratospheric intrusion at the subtropical jet over the Mediterranean Sea: air-borne remote sensing observations and model results. Atmos. Chem. Phys. 12, 8423–8438, doi: 10.5194/acp-12-8423-2012.

Winkler, R., Dietl, F., Frank, G., Tschiersch, J., 1998. Temporal variation of ^{7}Be and ^{210}Pb size distributions in ambient aerosol. Atmos. Environ. 32 (6), 983–991, doi: 10.1016/s1352-2310(97)00333-6.

Yoshimori, M., 2005. Beryllium-7 radionuclide as a tracer of vertical air mass transport in the troposphere. Adv. Space Res. 36, 828–832, doi: 10.1016/j.asr.2005.04.088.

Zanis, P., Gerasopoulos, E., Priller, A., Schnabel, C., Stohl, A., Zerefos, C., Gäggeler, H.W., Tobler, L., Kubik, P.Q., Kanter, H.J., Scheel, H.E., Luterbacher, J., Berger, M., 2003. An estimate of the impact of stratosphere-to-troposphere transport (STT) on the lower free tropospheric ozone over the Alps using ^{10}Be and ^{7}Be measurements. J. of Geophys. Res. 108 (D12), 8520, doi: 10.1029/2002jd002604.

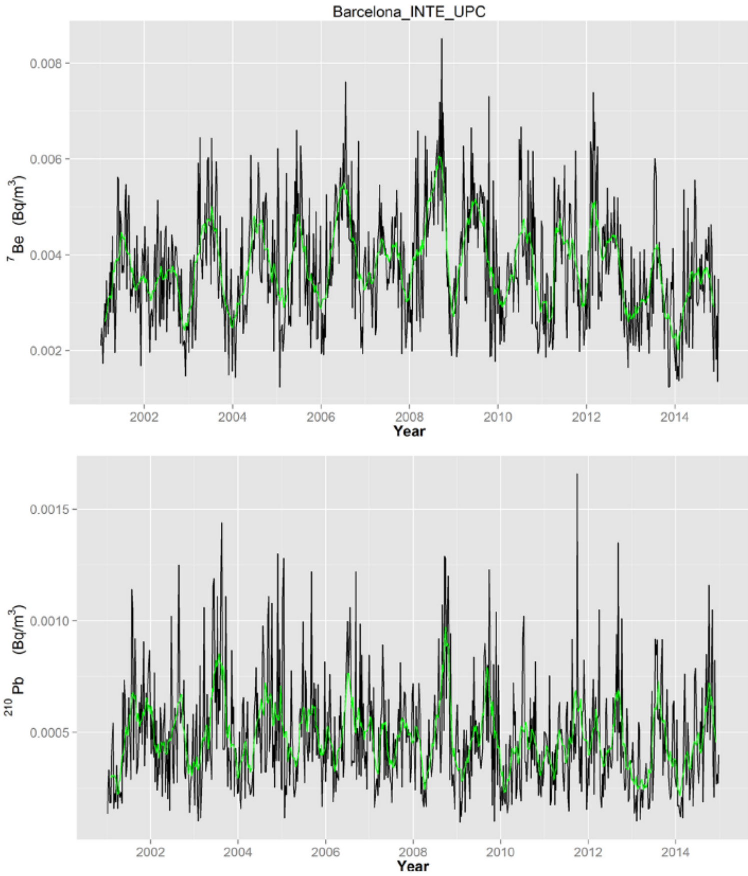

Fig. 1. Concentrations of atmospheric ^{7}Be (top) and ^{210}Pb (bottom) in the city of Barcelona. Green lines correspond to the 3-month moving average. (For interpretation of the references to colour in this figure legend, the reader is referred to the web version of this article.)

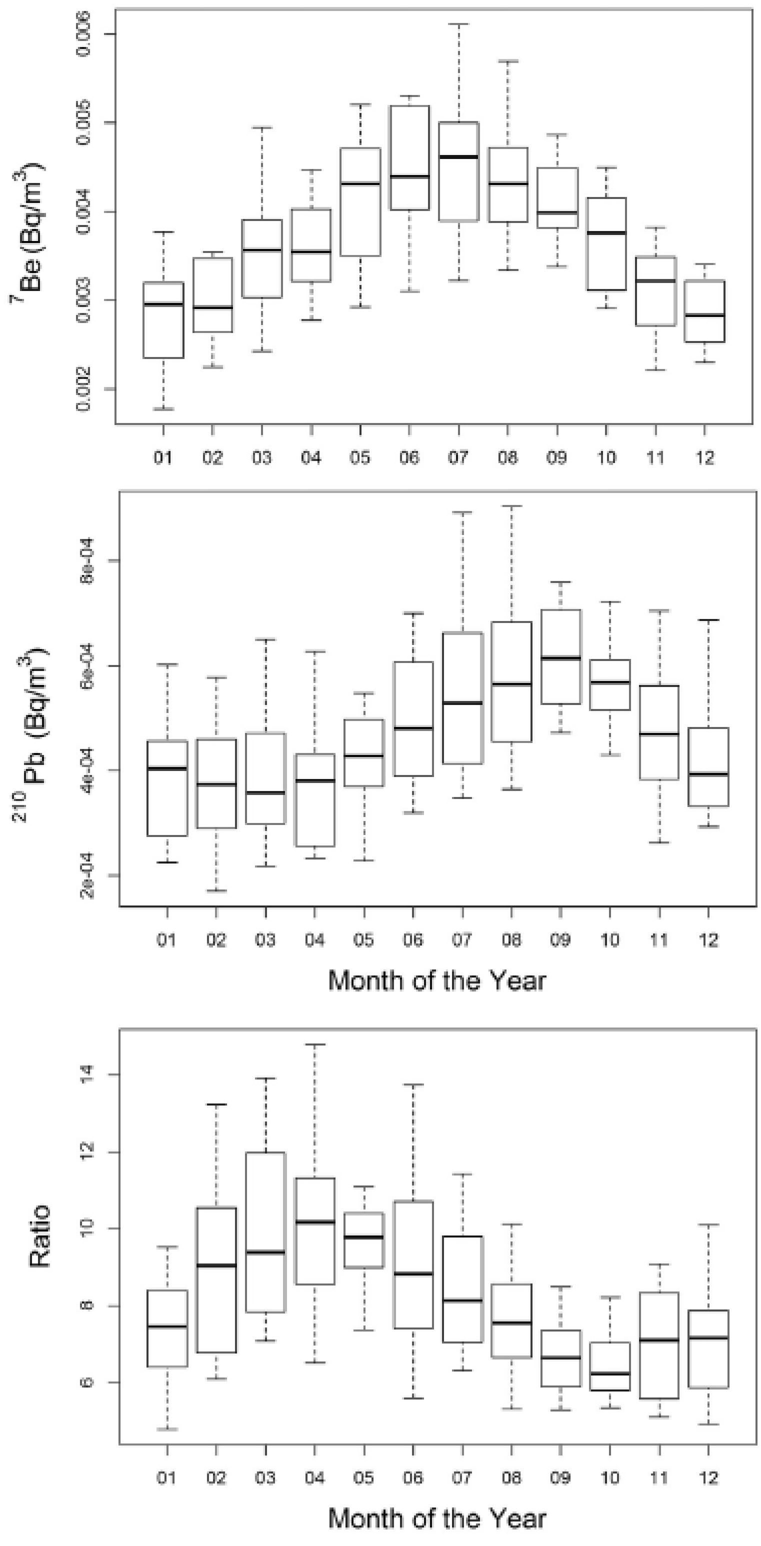

Fig. 2. Box plots of ^{7}Be (top), ^{210}Pb (middle) and the ratio ^{7}Be/^{210}Pb (bottom) for each calendar month. For each month the 25th (low box limit) and 75th (up box limit) percentiles are reported in the plot. The median (black line in the box), min and max values, described by the whiskers of each box, are also reported.

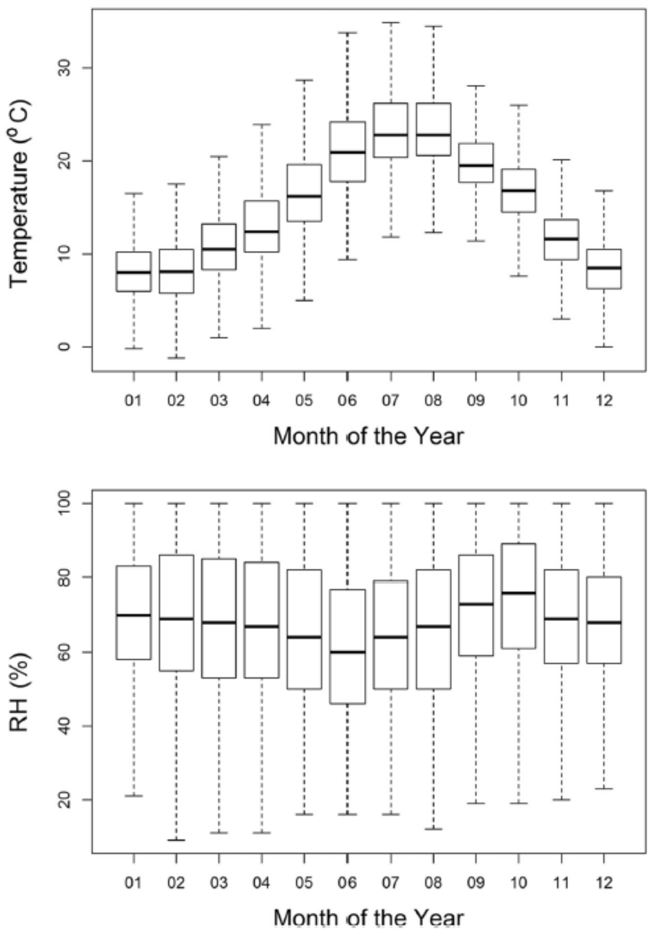

Fig. 3. Box plots of T (top) and RH (bottom) conditions for each calendar month. For each month the 25th (low box limit) and 75th (up box limit) percentiles are reported in the plot. The median (black line in the box), min and max values, described by the whiskers of each box, are also reported.

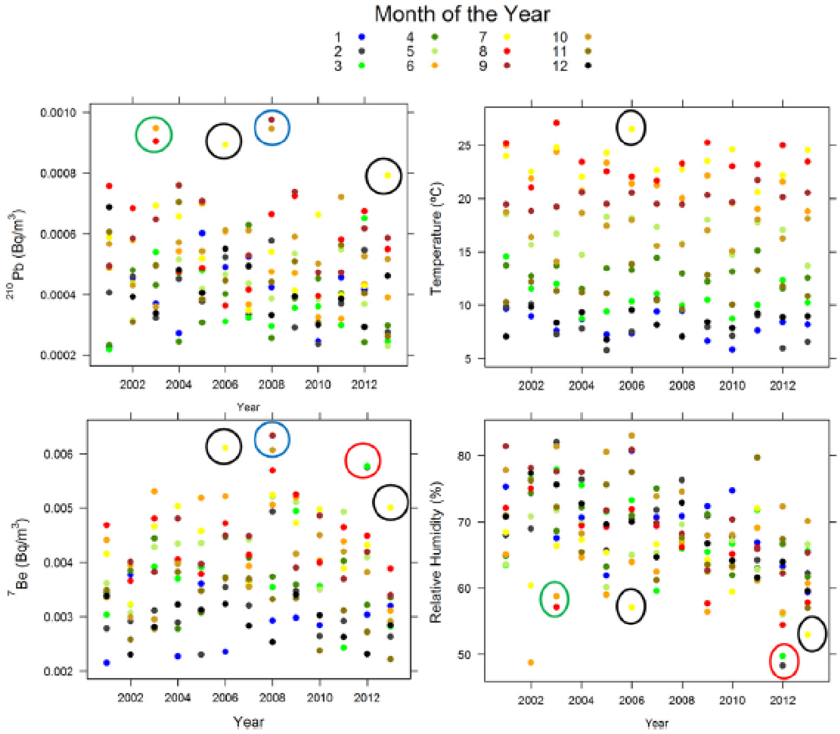

Fig. 4. Monthly values of ^{7}Be (down-left), ^{210}Pb (up-left), T (up-right) and RH (down-right) measured in Barcelona over 13 years data set.

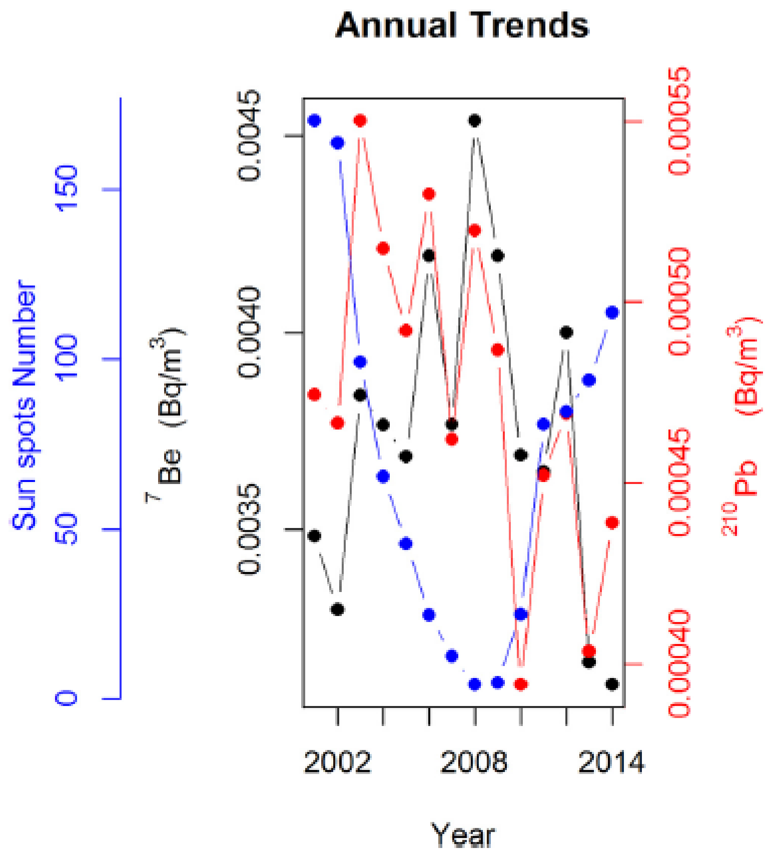

Fig. 5. Year-to-year variability of annual mean ^{7}Be (black), ^{210}Pb (red) and the number of sun spots (blue). (For interpretation of the references to colour in this figure legend, the reader is referred to the web version of this article.)

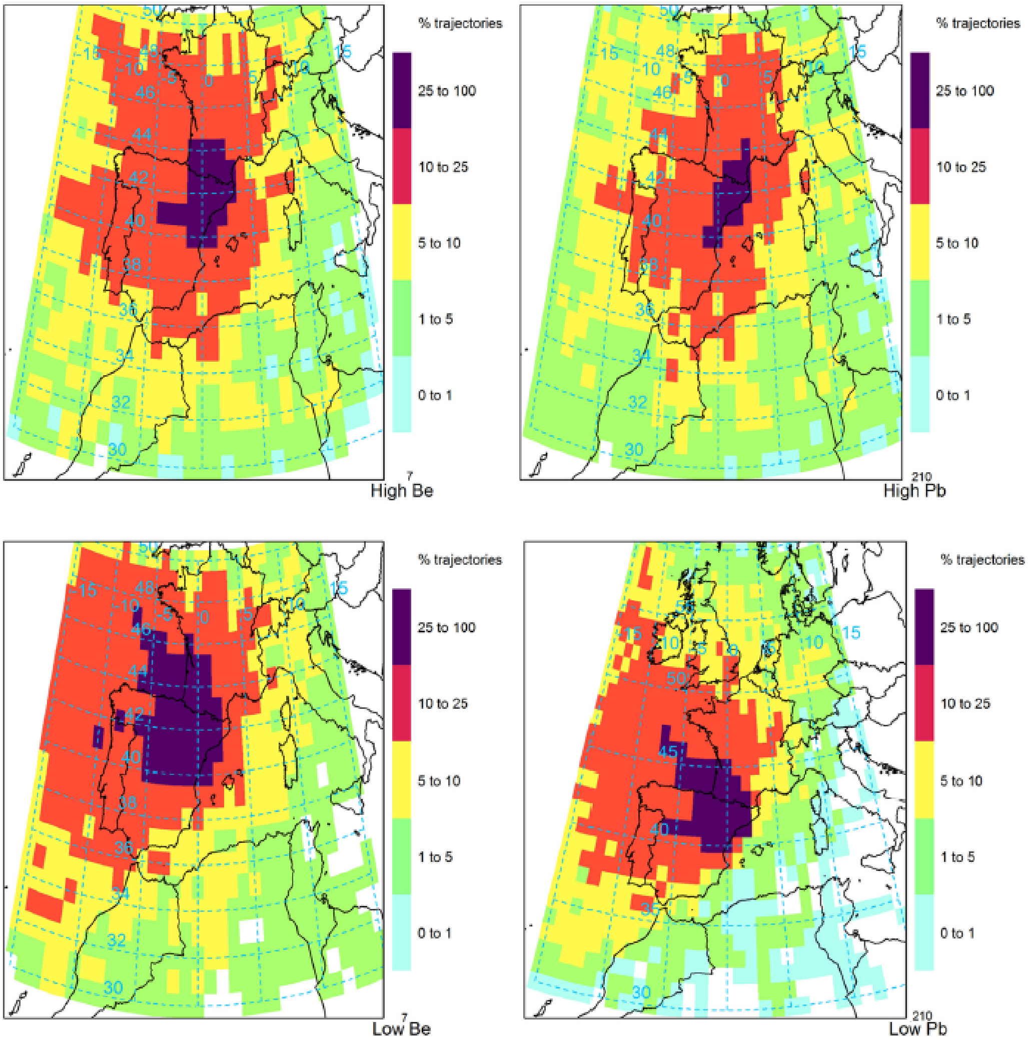

Fig. 6. Frequency maps of back trajectories for high (top) and low (bottom) values of ^{7}Be (left) and ^{210}Pb (right).

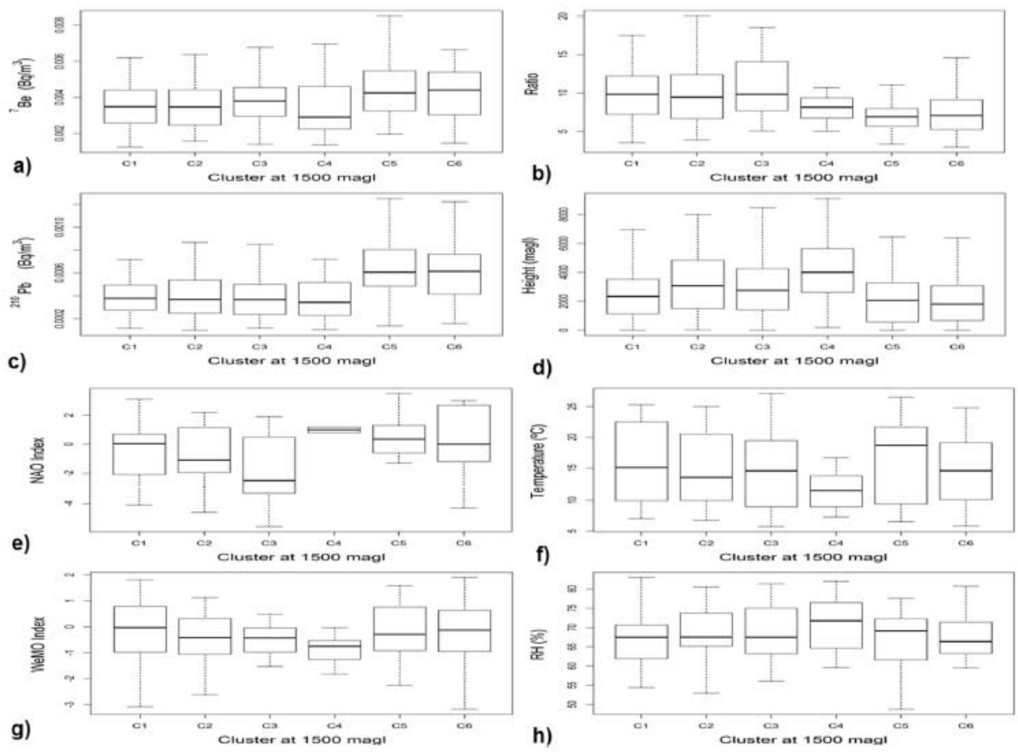

Fig. 7. Box plots of ^{7}Be, ^{210}Pb, origin height, $^{7}Be/^{210}Pb$, WeMO, NAO, T and RH for each cluster. For each month the 25th (low box limit) and 75th (up box limit) percentiles are reported in the plot. The median (black line in the box), min and max values, described by the whiskers of each box, are also reported.

Table 1
Spearman correlation values between ^{7}Be (t + h) and ^{210}Pb(t), with negative (positive) values of *h* when ^{7}Be leads to (is led by) ^{210}Pb.

	^{7}Be(t-4)	^{7}Be(t-3)	^{7}Be(t-2)	^{7}Be(t-1)	^{7}Be(t+0)	^{7}Be(t+1)
^{210}Pb(t)	0.13	0.33	0.37	0.42	0.65	0.17

Table 2
Back trajectories cluster, frequency of the cluster occurrence, means of ^{7}Be and ^{210}Pb concentrations (mBq m^{-3}) with their standard errors, Spearman correlations (and corresponding p-value) of monthly radionuclide concentrations, for each cluster, with monthly values of the NAO and WeMO indexes, and with monthly local T (°C) and RH (%) values in Barcelona.

Cluster	F (%)	^{7}Be	^{210}Pb	^{7}Be				^{210}Pb			
				NAO	WeMO	RH	T	NAO	WeMO	RH	T
C1_AOS	21	3.56 ± 0.09	0.40 ± 0.02	−0.09 (0.27)	**−0.21 (0.01)**	**−0.21 (0.01)**	**0.58 ($7.7 \cdot 10^{-14}$)**	−0.02 (0.77)	**−0.21 (0.01)**	−0.16 (0.07)	**0.44 ($7.9 \cdot 10^{-8}$)**
C2_NAM	17	3.52 ± 0.10	0.39 ± 0.02	0.10 (0.27)	**−0.21 (0.02)**	**−0.24 ($8.5 \cdot 10^{-3}$)**	**0.43 ($1.1 \cdot 10^{-6}$)**	0.02 (0.81)	**−0.22 (0.02)**	0.02 (0.84)	**0.23 (0.01)**
C3_NAS	16	3.80 ± 0.11	0.40 ± 0.02	−0.10 (0.28)	**−0.21 (0.03)**	−0.05 (0.61)	**0.41 ($1.3 \cdot 10^{-5}$)**	0.01 (0.89)	**−0.27 (0.004)**	0.16 (0.09)	**0.30 (0.01)**
C4_NAF	7	3.45 ± 0.19	0.41 ± 0.03	0.04 (0.76)	−0.03 (0.81)	−0.07 (0.62)	0.25 (0.08)	0.11 (0.46)	−0.22 (0.13)	−0.18 (0.21)	−0.03 (0.81)
C5_R	20	4.19 ± 0.11	0.61 ± 0.02	−0.06 (0.48)	−0.14 (0.11)	**−0.27 (0.01)**	**0.49 ($4.3 \cdot 10^{-9}$)**	0.005 (0.95)	−0.06 (0.50)	−0.02 (0.81)	**0.33 ($1.1 \cdot 10^{-4}$)**
C6_E	19	3.97 ± 0.10	0.59 ± 0.02	0.04 (0.62)	−0.14 (0.08)	**−0.22 ($8.9 \cdot 10^{-3}$)**	**0.48 ($9.2 \cdot 10^{-10}$)**	0.07 (0.37)	**−0.17 (0.03)**	−0.02 (0.83)	**0.32 ($9.6 \cdot 10^{-5}$)**

Bold indicates the highest correlations values.